Recovery and Operational Best Practices for Reaction Wheel Bearings

Michael J. Dube*, Jeff Fisher**, Stuart Loewenthal+ and Peter Ward++

Abstract

Left unaddressed, the observation of sustained high torque signatures in bearing applications ultimately leads to failure. This paper describes vacuum bearing testing of 40 motors fitted with R4 angular contact bearings with 52% and 54% race curvatures, in all steel and hybrid configurations, running in different lubrication regimes. Testing was intended to identify any differences in bearing performance attributed to operation and configuration, and evaluate approaches to recovering bearings in distress with the goal of restoring bearing performance. This paper will present data and describe approaches employed, including resting and heating, that have in some cases resulted in successful bearing recovery, avoiding the onset of hard failure and restoring performance for varying periods of time. Data addressing performance differences between motors equipped with all steel R4 bearings with 52% and 54% curvatures, as well as, performance differences between all steel bearings and their hybrid counterparts will be presented.

Introduction

Over the past decade, there have been several reaction wheel assembly (RWA) in-service bearing related failures. The Kepler spacecraft, launched in March 2009, experienced failures of two of its RWAs in 2012 and 2013 [1]. The Thermosphere Ionosphere Mesosphere Energetics and Dynamics (TIMED) satellite suffered an RWA failure in 2007. The Dawn space probe experienced failures of one of its reaction wheels in 2010 and another in 2012, and when a third reaction wheel stopped working in 2017, Dawn resorted to its hydrazine thrusters for attitude control [2]. Similarly, the Far Ultraviolet Spectroscopic Explorer (FUSE) spacecraft experienced three bearing-related RWA failures [3]. In the commercial sector, a second generation Globalstar satellite failed to spin up one of its RWAs, despite high torque commands. This event was attributed to a stuck bearing, and shortly after regaining control with the three remaining RWAs, a second RWA exhibiting a similar torque signature failed [4].

Efforts to maintain reaction wheel performance and extended life have included attempts at bearing recovery employing techniques such as rest, increasing temperature, and reversing direction. These actions have had limited success with reliance on the remaining reaction wheels as the only recourse. This approach suffers from the potential for similar life-threatening bearing related issues. As a result, the NASA Engineering and Safety Center initiated a multi-year assessment that included an extensive bearing test program to evaluate the failure modes and effectiveness of potential on-orbit recovery techniques for R4 bearings experiencing high torque arising from cage instabilities and lubricant depletion leading to failure. This investigation is one of the most comprehensive efforts of its kind with 40 test motors fitted with R4 angular contact duplex bearings in all stainless steel and hybrid (ceramic balls) configurations, tested in hard vacuum at 3 different test speeds and 2 different temperatures. Motors incorporating R4 bearings with 52% and 54% race curvatures were included because there is anecdotal evidence that tight ball-race curvatures can lead to early failure, a claim that to the best of our understanding has never been documented. In addition, the testing performed in this investigation and its associated findings are of value to designers of bearings for scanners, gimbals, and other rotary spacecraft actuators.

* NASA Langley Research Center, Hampton, VA

** Fisher Aerospace, Sunnyvale, CA

\+ Lockheed Martin Space (retired), Sunnyvale, CA

++ The Aerospace Corporation, El Segundo, CA

R4 Bearing Life-Testing

The initial test plan envisioned testing 40 brushless DC motors in thermal vacuum bell jar chambers that were available at NASA Marshall Space Flight Center (MSFC) [5]. The large number of motors selected was an attempt to obtain statistically relevant life-test data while discerning any effects on bearing life attributed to race curvature, speed, temperature, and mode of operation. Additionally, we were interested in evaluating the differences in performance between all steel and hybrid (ceramic balls) bearings.

Motor Selection

Motor selection was driven by the size of the bell jars and the chiller plates that they could accommodate. Our focus was placed upon procuring vacuum compatible test motors that could easily incorporate our ABEC-7, angular contact, R4 size, 440C bearings and accommodate the existing test rigs at NASA MSFC. Special vacuum and cleanroom processes were imposed on the motor structural parts and windings, as well as, the capability to set the same bearing preload regardless of race curvature or ball material (steel or ceramic). We approached a high-volume production motor supplier willing to accommodate our custom requirements and selected 3-phase brushless DC motors with encoders to provide accurate speed control. Shaft and housing were modified for our R4 test bearings to establish proper fits over a test temperature range from ambient to 60°C. The bearings were preloaded with a wave washer that could be adjusted for each motor to meet the target bearing preload of 2.9 ± 0.23 kg (6.5 ± 0.50 lb) using a force gauge. The 2.9-kg preload approximates the mean contact stress of approximately 8.55e8 Pa (124 ksi) of flight RWA steel bearings (Figure 1). The motors had strip heaters with thermocouples mounted on the rear portion of the housing.

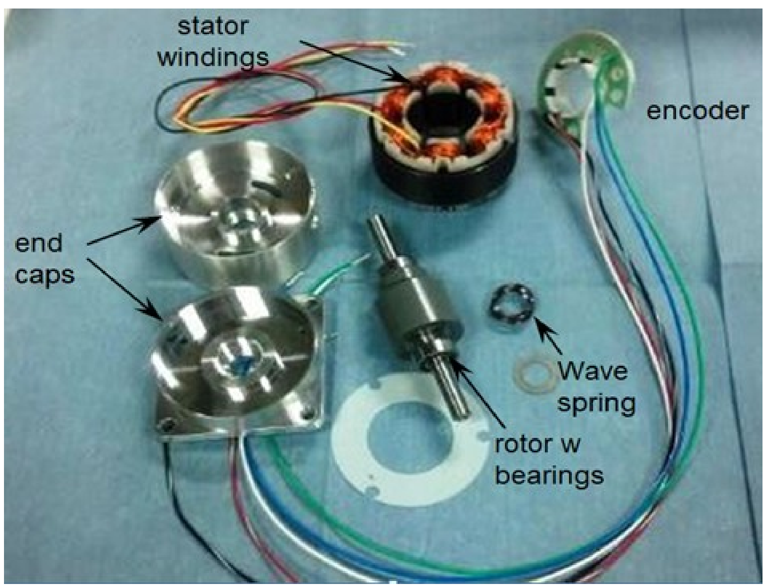

Figure 1. Test motor showing component parts (strip heaters and bearings not shown).

Lubrication

There was an expectation that the test motors would have extremely long lifetimes if the bearings were nominally lubricated [6]. In an attempt to minimize test time, the bearings were lubricated with a minimal amount of Nye Synthetic Oil 2001. The procedure used to effect this outcome involved immersing an oil lubricated bearing in an oil-solvent mixture followed by evaporation of the solvent until a very small meniscus was observed as determined visually under a microscope (Figure 2). This procedure was referred to as 7% lubricant slosh. The final bearing weights were measured and the variation found to be acceptable and typical of bearing to bearing variation in the field. One exception to performing this procedure was motor 40 which received a 3% lubricant slosh where a meniscus was not observed. This exception was to reproduce the lubrication condition present in a prototype test that was run previously in an all steel configuration.

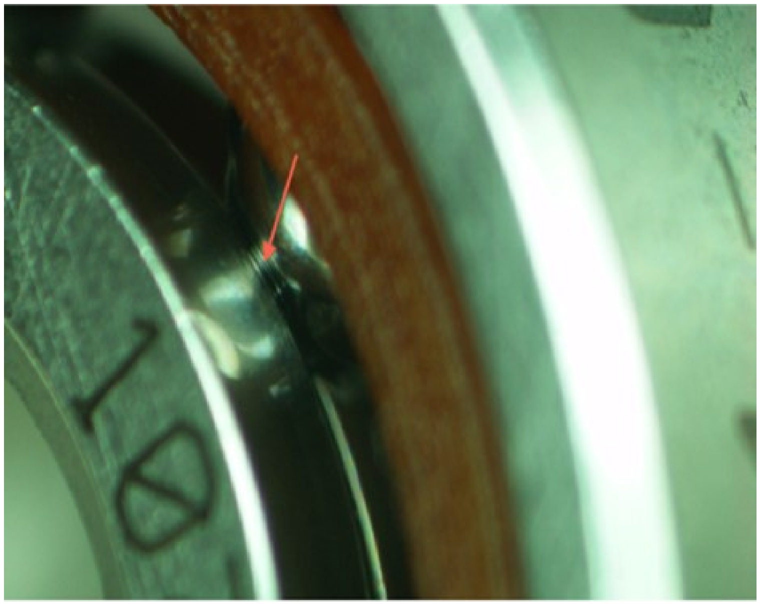
Figure 2. Oil meniscus present in R4 Bearing after 7% lubricant slosh (Nye Synthetic Oil 2001/heptane).


Figure 3. Test motors mounted on chiller plate and installed in bell jar.

<u>Phase I Testing</u>
The motors were divided into three sets, mounted on chiller plates, and each set placed in a vacuum bell jar (Figure 3). Two bell jars labeled Bell Jars #1 and #2 contained 16 motors each and had all steel bearings, while a third bell jar labeled Bell Jar #3 contained 8 motors and had hybrid bearings. Each bell jar contained motors possessing both 52% and 54% bearing curvatures. Phase I testing consisted of all motors running

at 60°C and 314 rad/s (3000 rpm). These conditions were selected to accelerate the test and introduce a large number of bearing revolutions and associated stress cycles on the lubricant by operating in the boundary lubrication regime. Current from the DC test motors was converted to bearing torque to track and trend the health of the bearings. The baseline torque was comprised of bearing plus motor torque, and was recorded at the beginning of the life test and monitored throughout the testing with any observed increases in torque attributed to bearing drag since the motor torque was constant over time.

Phase II Testing

Phase II testing was initiated shortly after the failure of motor 22 (52% curvature) which took place at 436 million revolutions (Figure 4). The temperature control for Bell Jars #1 and #2 was first lowered to a plate temperature of 45°C, temporarily, to avoid any potential damage due to dropping the temperature too quickly, then adjusted to 25°C resulting in motor temperatures ranging from 26-28°C. The final plate temperature of 25°C was selected to operate the motors at a temperature more typical of RWAs in flight. At this point, the motors with all steel bearings were categorized into two groups based on curvature and the operating mode of each group subcategorized and adjusted as follows: 1.) 105 rad/s (1000 rpm) no zero crossings, 2.) 105 rad/s (1000 rpm) with zero crossings, 3.) 52.4 rad/s (500 rpm) no zero crossings, 4.) 52.4 rad/s (500) rpm with zero crossings. The motors with hybrid bearings were allowed to continue running at 314 rad/s (3000 rpm) and 60°C until they achieved ~5.3 billion revolutions where the temperature and speed on the hybrid motors was adjusted to 27-29°C and 105 rad/s (1000 rpm), respectively, with pairs running with and without zero crossings. A summary of the testing configuration is shown in Figure 5. The speed was reduced periodically to 31.4 rad/s (300 rpm) on all motors then ramped up to set speed in order to estimate the coulombic and viscous components of friction comprising the total torque. The viscous component was extrapolated to 314 rad/s (3000 rpm) for the motors running at 105 rad/s (1000) and 52.4 rad/s (500 rpm). This measurement was useful in tracking the state of lubrication in the bearings over time since the viscous component of friction would slowly decrease while the coulombic friction would increase, providing an indication that the lubricant was being depleted. Microphones were added to detect any noise associated with cage instabilities. In some cases, as the bearings reached end of life, the total torque would suddenly step-up (Figure 6) with the bell jar microphones recording an increase in the background noise. One example where the background sound amplitude increased 12 to 20 dB in the 1400 to 2400 Hz range, a signature indicative of a bearing experiencing dry cage instability, is shown in Figure 7.

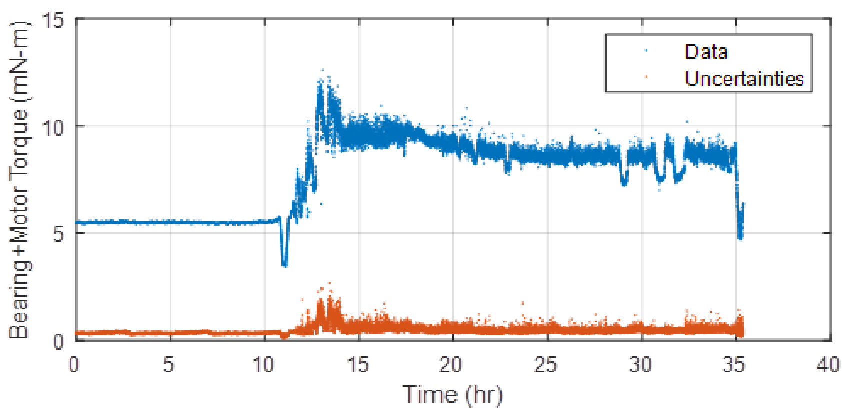

Figure 4. Motor 22 torque signature at point of failure in phase I testing (436 million revolutions).

Results

The testing described in this paper has been running for over 4 years. There have been four 440C and two hybrid bearing failures and one motor with 440 C bearings fully recovered. Hybrid motor 40 testing was suspended when its torque versus speed curve showed no viscous response. All of the steel bearing failures, occurred at less than 1.4 billion revolutions, whereas the hybrid bearing failures in motors 33 and 36 occurred at greater than 5.3 billion revolutions, a significant finding in this work. It is important to note that motor 22, with all steel bearings, and motors 33 and 36, with hybrid bearings, were all running under identical conditions (314 rad/s, 60°C) at the time of their respective failures. See Figure 5 and Table 1.

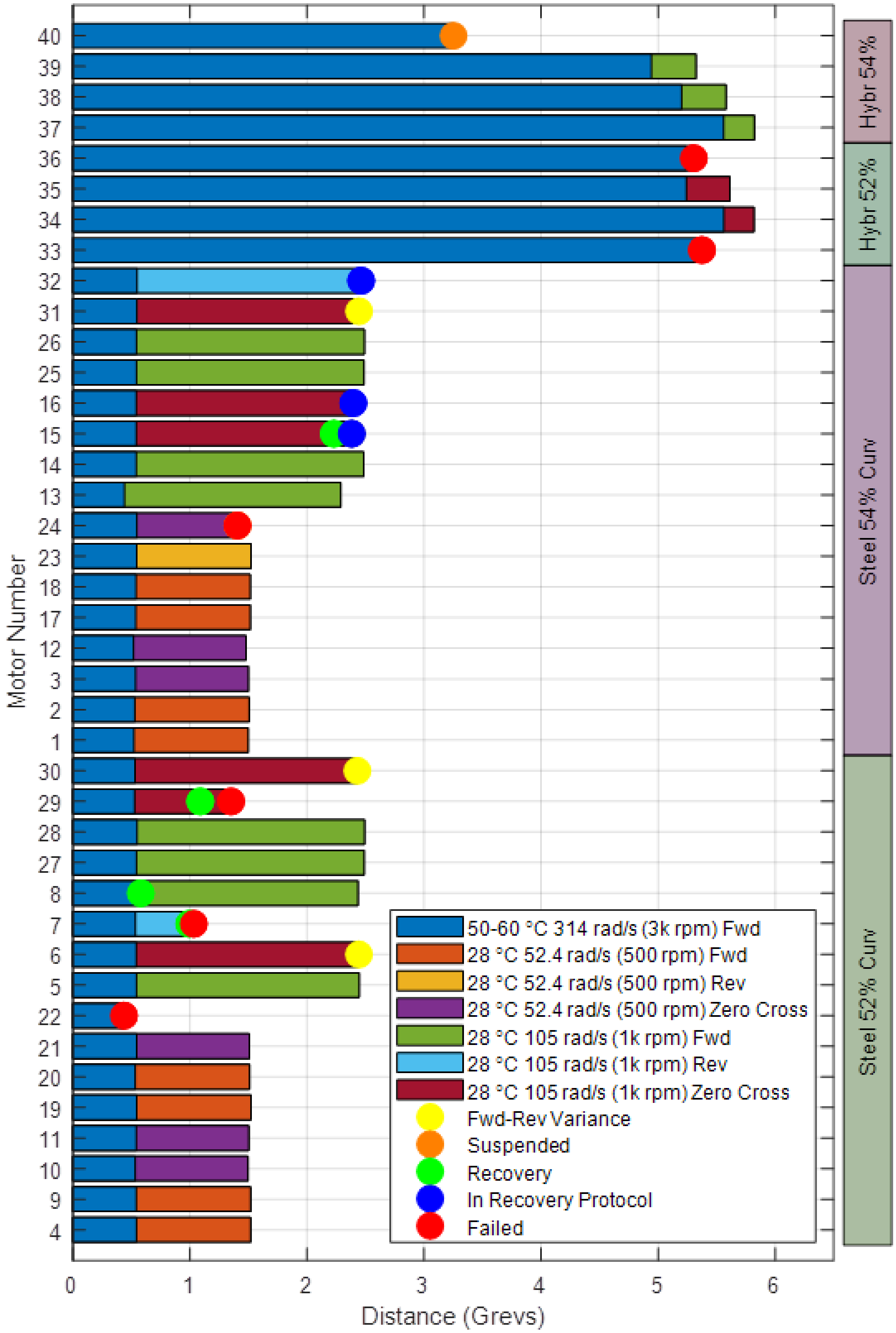

Figure 5. Summary of motors in test and results acquired to date.

Table 1. Summary of Motor and Bearing Results

Steel Bearings					
Motor	**Curvature (%)**	**Failure (revolutions)**	**Speed (rad/s)**	**Mode**	**Recovery**
22	52	4.36e6	314 (3000 rpm)	biased	No
8	52	5.79e6	105 (1000 rpm)	biased	Full
7	52	9.95e6	105 (1000 rpm)	biased	No
29	52	1.09e9/1.34e9	105 (1000 rpm)	zero crossings	Yes/No
24	54	1.36e9	52.4 (500 rpm)	zero crossings	No
Hybrid Bearings					
Motor	**Curvature (%)**	**Failure (revolutions)**	**Speed (rad/s)**	**Mode**	**Recovery**
40	54	3.25e9	314 (3000 rpm)	Biased	Suspended
36	52	5.30e9	314 (3000 rpm)	biased	No
33	52	5.37e9	314 (3000 rpm)	biased	No

Hybrid Motors

Hybrid motors 33 and 36 were shut down to evaluate recovery techniques. The torque signature and acoustic data for motor 33 were consistent with bearing dry cage instability as shown in Figures 6 and 7, respectively. One motor was rested for 37 days then run another 45 hours before suffering a probable cage failure. The other motor with hybrid bearings was also rested for 37 days and then heat soaked at 60°C for another 30 days when it failed from probable cage fracture after 7 hours of additional operation (Table 1). Neither motor with hybrid bearings has been torn down for inspection to validate the failure mode so as not to disturb the remaining motors under test.

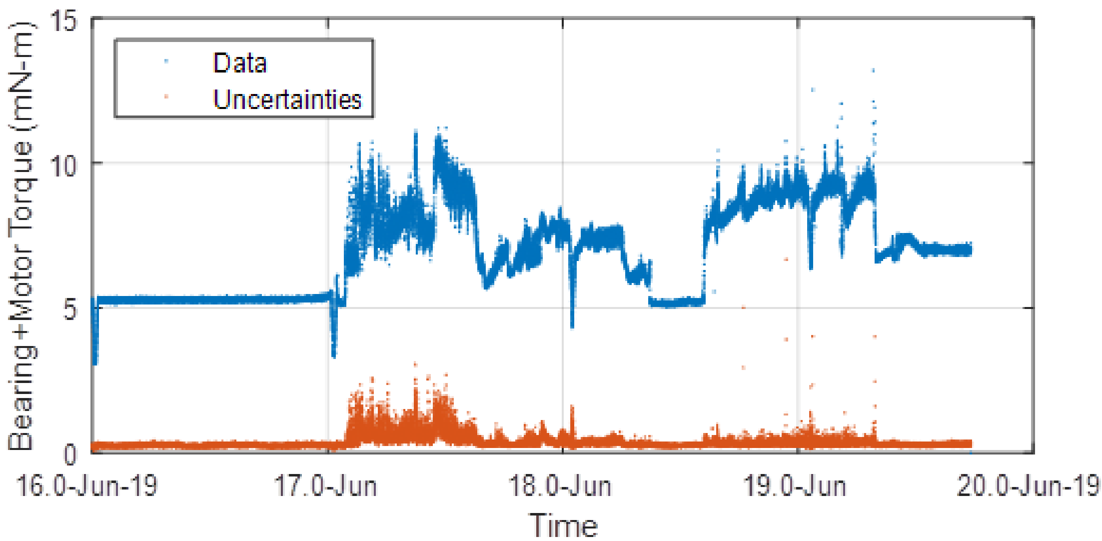

Figure 6. Motor 33 torque signature for dry cage instability.

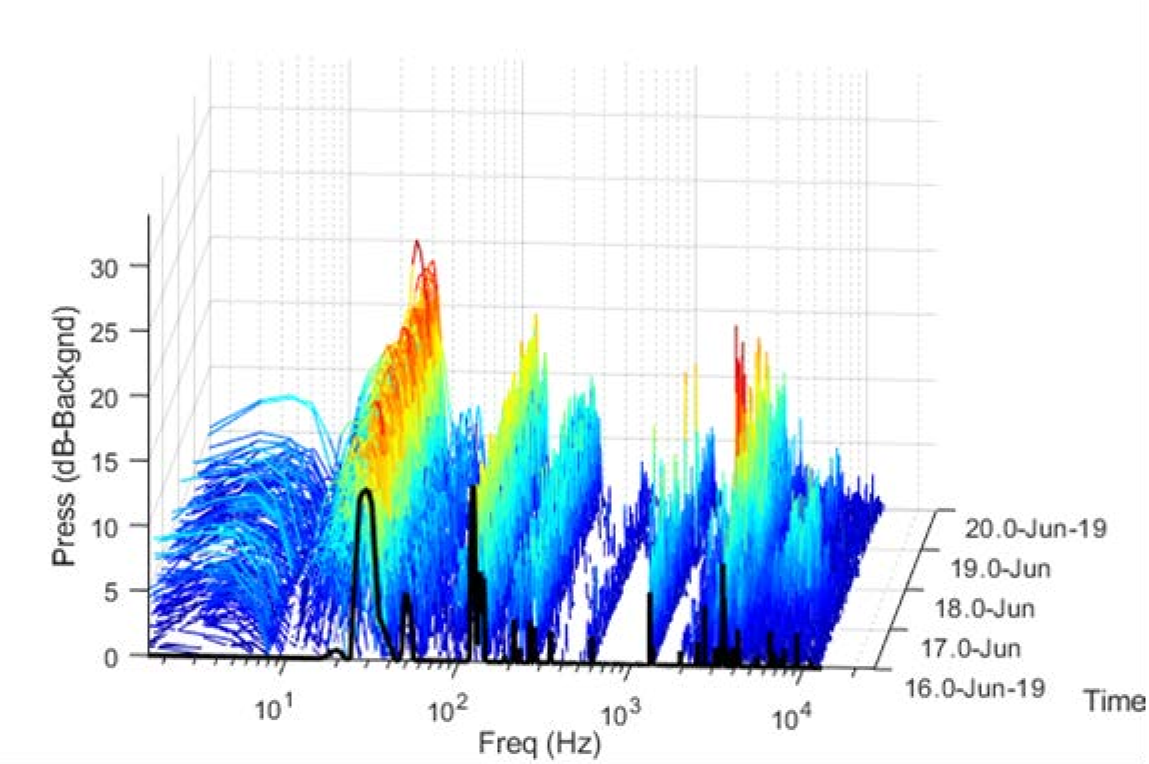

Figure 7. 12-20 dB spikes between 1400-2400 Hz associated with dry cage instability on motor 33.

As mentioned earlier, and as shown in Table 1, motor 40 with hybrid bearings was suspended at 3.25e9 revolutions. This motor was run at 314 rad/s and 50°C to approximate conditions that were run previously in prototype testing where the motor in an all steel configuration failed at ~250 million revolutions. Note that motor 40 was lubricated with a 3% slosh and did not have a visible meniscus. As can be seen in Figure 8, the Coulombic torque increased as the viscous torques decreased. These coincident events were clear indications that the lubricant was depleted and the bearing was running in a "dry" condition. Further operation likely would have triggered a dry cage instability and eventual cage fracture, and it was for these reasons that the test was suspended in order to preserve the motor for eventual teardown and inspection.

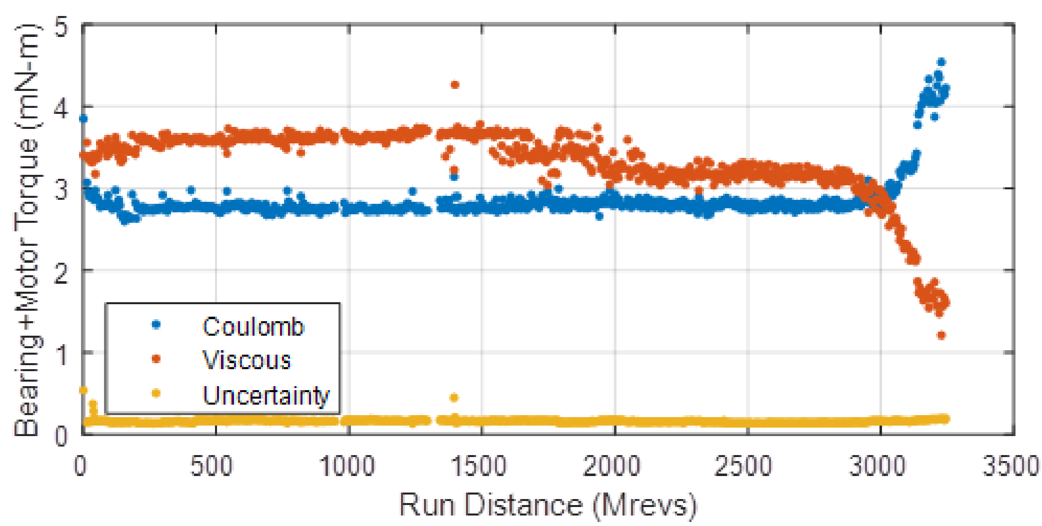

Figure 8. Plot of viscous and Coulombic torque versus distance.

<u>Steel Motors</u>

The same recovery techniques were applied to motors 7 and 29 with all steel bearing configuration and which failed at approximately 1 billion revolutions. They were rested 37 days at ambient and then heat soaked. Motor 7 reversed direction 5 times and was rested for a total of 227 days with no signs of improvement. Motor 29 was rested for 37 days then heat soaked unpowered at 60°C for an additional 30 days with the motor recovering for approximately 260,000 revs before failing again. Remarkably, motor 8 with all steel bearings showed high torques at 579 M revs and was rested at ambient for 37 days. It then recovered fully, and is currently healthy at 2.2 B revs while performing zero speed crossings (Figure 9).

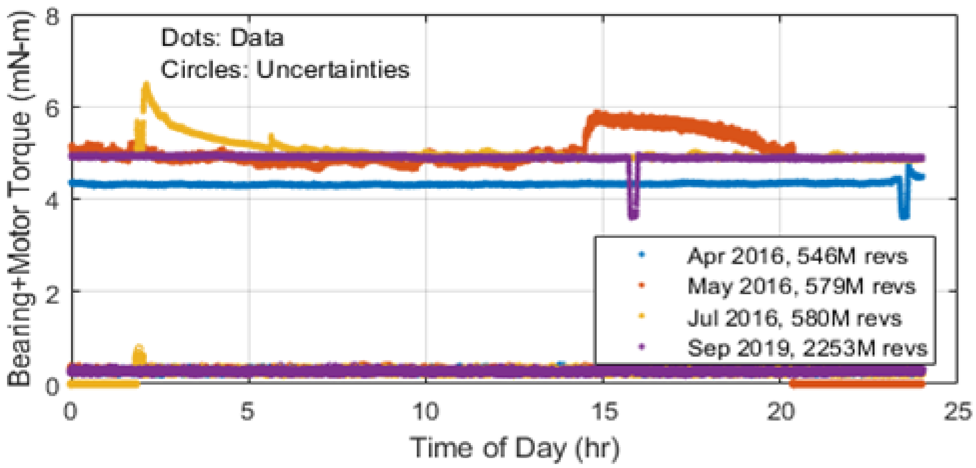

Figure 9. Typical day before failure (blue), failure event (orange), restart (gold) and recovery (purple).

<u>Motors in Recovery Protocol</u>

Motor 15 exhibited anomalous torque spikes at 2.23 billion revolutions, was rested for 42 days, and recovered for 30 days upon which time torque spikes were observed again and the motor rested and subjected to a heat soak. Motor 16 also exhibited torque spikes at 2.28 billion revolutions at which time it was shut down and rested. Motors 15 and 16 were not considered failures as recovery was attempted. In contrast, motor 32 exhibited behavior consistent with dry cage instability and was shut down and subjected to a 37-day rest period. Motors 15, 16, and 32 all possessed 54% curvature. The results of the recovery protocol imposed on motors 15, 16, and 32 were not yet available at the time of writing this paper as shown in Figure 5.

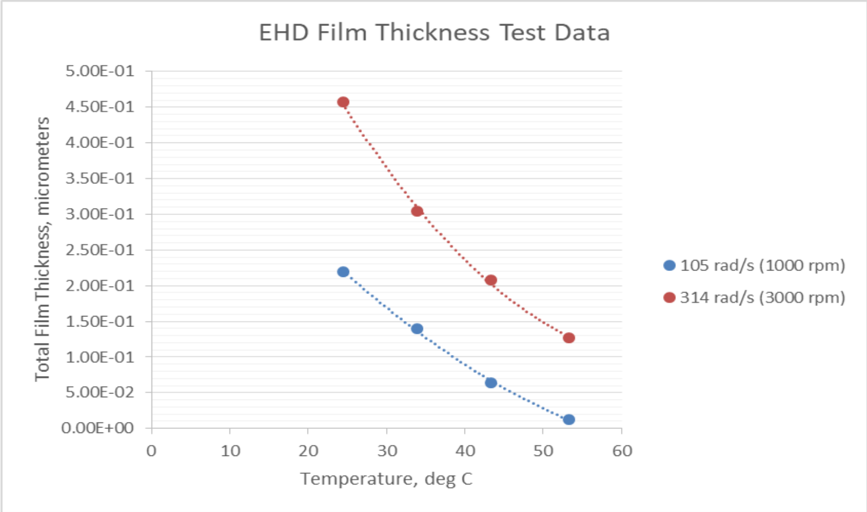

Figure 10. Film thickness versus temperature at 314 rad/s and 105 rad/s.

Conclusions

The testing described in this paper will continue since only 6 of the 40 test motors have failed. Post-test inspection to confirm failure modes will also be performed. At this point in the investigation, some key preliminary findings have emerged (Figure 5 and Table 1):

1) Of the four 440C and two hybrid bearing failures, five of the six failed motors had bearings with 52% race curvature suggesting that tight curvatures, while improving load capacity, may possess shorter life. It has long been suspected that tight curvatures can lead to torque irregularities adversely affecting bearing lubricant life [7]. While our results are preliminary, this study may be the first to quantitatively confirm this point.
2) To date, only one out of the four motors that failed with all steel bearings occurred at 52.4 rad/s (500 rpm). The other three failures occurred at 105 rad/s (1000 rpm). Of the 16 motors that have been running at 105 rad/s (1000 rpm), three are currently in recovery protocol, three have failed, and one has fully recovered. There has been only one motor failure out of the 15 motors running at 52.4 rad/s (500 rpm). Although, bearings running at the 105 rad/s (1000 rpm) had roughly twice the running distance at the time of failure as their 52.4 rad/s (500 rpm) counterparts, it is interesting to point out that the failures of motors that were running at 105 rad/s (1000 rpm) occurred at total revolutions less than currently observed for the 14 motors still running at 52.4 rad/s (500 rpm). Bearings running at 52.4 rad/s (500 rpm) have less favorable lubricant film thickness and should theoretically fail sooner.
3) Hybrid bearings exhibited smoother, steadier torque signatures and achieved longer lives compared to the 440C bearings. Of particular note, motor 22 with 52% curvature and all steel configuration failed at 436 million revolutions while running under the same conditions as motors 33 and 36 with hybrid bearings which failed at 5.37 and 5.30 billion revolutions, respectively, providing a direct comparison between the performance of steel bearings and hybrid bearings of equivalent curvature.
4) All hybrid motors achieved an excess of 5 billion revolutions with only two failures, while the remaining 5 hybrid motors are still running. One motor with hybrid bearings, motor 40 (Figure 8), was suspended prior to the onset of failure in order to prevent dry cage instability and eventual cage failure. It is important to note that prior to initiating phase I motor 40 was previously run in prototype testing in an all steel configuration at 105 rad/s (1000 rpm) and 30°C where it failed ~250 million revolutions and resulted in a broken cage due to dry cage instability. While the conditions of operation differed, the 314 rad/s (3000 rpm) and 50°C conditions selected for motor 40 in phase I and phase II testing approached the same lubrication regime affording an indirect comparison of motors with steel bearings versus hybrid bearings (Figure 10).

References

1. Kampmeier, J. L., Larsen, R. J., Miglorini, L.F., Larson, K.A., “Reaction Wheel Performance Characterization Using the Kepler Spacecraft as a Case Study”, 2018 Space Operations Conference, 28 May-1 June, 2018, Marseille, France.
2. Bruno, D., “Contingency Mixed Actuator Controller Implementation for the Dawn Asteroid Rendezvous Spacecraft,” AIAA 2012-5289, AIAA SPACE 2012 Conference & Exposition, 11-13 September 2012, Pasadena, CA.
3. Sahnow, D. J. et al, “Operations with the New FUSE Observatory: Three-Axis Control with One Reaction Wheel,” *SPIE Proceedings, Vol. 6266, July 2006*.
4. Hacker, J. M., Goddard, J. L., and Lai, P. C., “Globalstar Second Generation Hybrid Attitude Control On Orbit Experience,” AAS 14-454, 24th AAS/AIAA Space Flight Mechanics Meeting, Santa Fe, NM, 26-30 January, 2014.
5. McMurtrey, Ernest L., Lubrication Handbook for the Space Industry. Part A: Solid Lubricants. Part B: Liquid Lubricants. NASA TM-86556, December 1985.
6. Jones, William R; Jr., Jansen, Mark J., ”Lubrication for Space Applications,” NASA CR-2005-213424, 2005.

7. Loewenthal, Stuart L., "Two Gimbal Bearing Case Studies," Proceedings of the 22nd Aerospace Mechanisms Symposium, May 1988, NASA CP-2506.